electronics

MDPI

Article

Electrochemical Impedance Spectrum Equivalent Circuit Parameter Identification Using a Deep Learning Technique

Asier Zulueta [1], Ekaitz Zulueta [2], Javier Olarte [3], Unai Fernandez-Gamiz [1], Jose Manuel Lopez-Guede [2,*] and Saioa Etxeberria [4]

[1] Department of Energy Engineering, University of the Basque Country (UPV/EHU), 01006 Vitoria-Gasteiz, Spain; azulueta005@ikasle.ehu.eus (A.Z.); unai.fernandez@ehu.eus (U.F.-G.)
[2] Department of System Engineering and Automatic Control, University of the Basque Country (UPV/EHU), 01006 Vitoria-Gasteiz, Spain; ekaitz.zulueta@ehu.eus
[3] Centre for Cooperative Research on Alternative Energies (CIC EnergiGUNE), Basque Research and Technology Alliance (BRTA), Alava Technology Park, Albert Einstein 48, 01510 Vitoria-Gasteiz, Spain; jolarte@bcaremb.com
[4] Department of Mechanical Engineering, University of the Basque Country (UPV/EHU), 01006 Vitoria-Gasteiz, Spain; saioa.etxebarriab@ehu.eus
* Correspondence: jm.lopez@ehu.eus; Tel.: +34-945014084

Abstract: Physical models are suitable for the development and optimization of materials and cell designs, whereas models based on experimental data and electrical equivalent circuits (EECs) are suitable for the development of operation estimators, both for cells and batteries. This research work develops an innovative unsupervised artificial neural network (ANN) training cost function for identifying equivalent circuit parameters using electrochemical impedance spectroscopy (EIS) to identify and monitor parameter variations associated with different physicochemical processes that can be related to the states or failure modes in batteries. Many techniques and algorithms are used to fit a predefined EEC parameter, many requiring high-human-expertise support work. However, once the appropriate EEC model is selected to model the different physicochemical processes associated with a given battery technology, the challenge is to implement algorithms that can automatically calculate parameter variations in real time to allow the implementation of estimators of capacity, health, safety, and other degradation modes. Based on previous studies using data augmentation techniques, the new ANN deep learning method introduced in this study yields better results than classical training algorithms. The data used in this work are based on an aging and characterization dataset for 80 Ah and 12 V lead–acid batteries.

Keywords: neural networks; deep learning; electrical equivalent circuit; electrochemical impedance spectroscopy; model-based estimators; lead–acid batteries

Citation: Zulueta, A.; Zulueta, E.; Olarte, J.; Fernandez-Gamiz, U.; Lopez-Guede, J.M.; Etxeberria, S. Electrochemical Impedance Spectrum Equivalent Circuit Parameter Identification Using a Deep Learning Technique. *Electronics* **2023**, *12*, 5038. https://doi.org/10.3390/electronics12245038

Academic Editors: Yi Xie, Dan Dan and Jiahao Liu

Received: 26 September 2023
Revised: 24 November 2023
Accepted: 27 November 2023
Published: 18 December 2023

1. Introduction

The lecture notes and recordings in *ECE4710/5710: Modeling, Simulation, and Identification of Battery Dynamics* provide a 360° view of the modeling techniques used in batteries [1]. Research has been conducted to apply deep learning (DL) techniques to battery analyses, such as in [2,3], although there are also research studies based on more conventional neural networks, such as in [4,5]. Even more conventional algorithms such as the extended Kalman filter (EKF) are suitable for when battery state predictions must be calculated in real-time applications [6]. A detailed review of machine learning applications in battery state analyses can be found in [7].

Physical models are suitable for the development and optimization of materials and cell designs, whereas models based on experimental data and electrical equivalent circuits (EECs) are suitable for the development of operation estimators, both for cells and batteries. A good example of physical models applied to battery design can be seen in [8].

The most basic EECs consist of a voltage source in series with a resistor, representing the open-circuit voltage and the internal resistance of the cell, respectively. Additional R-C-scale series are often added to simulate the charge and mass transfer phenomena occurring at and around the electrolyte–electrode interface.

One method for selecting the equivalent circuit is to simulate different operating conditions. Then, the parameterization of the electrical components that constitute the circuit is usually performed using experimental voltage and current measurements [9,10]. Another option is using impedance spectroscopy [10]. Spectroscopy is easier to perform and more accessible. However, due to the variable nature of the R-C network components concerning the operating conditions (the state of charge (SOC), temperature, flow rate, and current), the parameterization process becomes a cumbersome task. The wider the operating window and the higher the desired accuracy, the greater the amount of experimental data required and the more complex the algorithms needed to perform the dynamic parameterization.

The association or determination of an EEC for a spectrum allows to have a model of the behavior of the battery where different components of the circuit are identified at each frequency range, as detailed by [11].

Electrochemical impedance spectroscopy (EIS) can be used for real-time predictions by interpreting parameters from spectra [12]. Battery EIS data represent a very powerful tool for identifying battery EEC models, which help to evaluate different battery states and in operando conditions. However, initially, the electrochemical model is difficult to implement and is very technology-specific, as described in the study by Piller et al. [13]. Therefore, it is necessary to develop specific protocols for extracting EIS measurements for each type of electrochemical energy storage technology, as demonstrated by Meddings et al. [14]. The identification process for an EEC to be extracted from EIS measurements usually requires human expertise complementary to support-specific software such as Zview, which offers impedance- or gain-phase graphing tools and guided circuit selection advice, as seen in the study by Csomós et al. [15]. Good reviews of the remaining battery life prediction techniques are presented in [16,17].

Additionally, the continuous monitoring of EIS data allows for adjusting and improving the accuracy of EEC models based on continuous models by allowing the identification of the initial conditions, as identified by Olarte et al. in [12].

Artificial neural networks (ANNs) have been widely used in the development of battery models for diagnosis and prognosis, as reported by Lombardo et al. [8]. In their work, the authors applied NNs to parameter identification because of the NNs' ability to fit non-linear relationships between inputs (EIS data) and outputs (equivalent circuit parameters), as demonstrated in the study by Chun et al. [18]. A related study can be found in [19]. Researchers have proposed a new loss function to train a neural network for EEC parameter predictions. Jimenez-Bermejo et al. [20] used NNs to obtain a more accurate estimation of the battery SoC in electric vehicles, and Yang et al. [21] used backpropagation (BP) NNs to estimate the battery SoH in electric vehicles, using a large amount of experimental data to feed the NNs.

ANNs can identify complex non-linear relationships between inputs (experimental EIS data, in our case) and outputs (EIS parameters, in our case). However, ANNs require extensive amounts of data to identify complex relationships because the architecture and number of weights are very large in these cases. Obtaining experimental data for all battery operating conditions is very time-consuming; therefore, we propose that an NN be trained with an initial set of real EIS data augmented with synthetic data corresponding to normal values for the equivalent circuit model. We emphasize the possibility of reducing the amount of experimental data by more efficiently generating synthetic data. This data augmentation process must be carefully carried out, since the EEC parameters are very dependent on each other, meaning it is not possible to achieve complete stochastic data augmentation. As such, we propose that a feasible data augmentation process is conducted via an experimental data comparison.

A two-step parameter identification algorithm to monitor EEC parameter variations was reported in a publication by Olarte et al. [22]. The authors' goal with the proposed method was to automatically monitor the variations in the EEC parameters in operation with impedance sensors to infer the variations in the battery health state or failure modes from the electrochemical interpretation of these values, as in the study by Chun et al. [18].

In this work, we propose a new deep learning (DL) technique for identifying an equivalent circuit's parameters from a series of EIS data using a trained ANN. Once the ANN is trained, algorithms of very low computational complexity can be implemented, allowing the design of systems for economically monitoring the evolution of the EEC parameters associated with the battery states.

The structure of this paper is as follows. Section 2 poses the target problem, providing the foundations and addressing the solution. The method proposed to directly learn the model from the EIS data is provided in Section 3. Section 4 reports the obtained results, while Section 5 discusses the results. Finally, Section 6 presents our conclusions.

2. EEC Parameter Identification Problem

Here, we propose a new DL NN-based algorithm that predicts an equivalent circuit's parameters via EIS, as defined in Section 2.1. To achieve this objective, we designed a new training loss function that forces the ANN to propose an equivalent circuit's parameter set (see Tables 1 and 2) that explains the EIS data as well as possible (see Section 2.2). The variables defined in the mathematical model are presented in Table 3.

Table 1. Parameters extracted from EIS spectra by adjusting the Zview software (initial raw data for the batteries in one of six rounds of essays).

SoC	R1	CPE1T	CPE1P	R2	CPE2T	CPE2P	R3
100%	0.0027176	7.17	0.85729	0.0092174	87.18	0.65421	-
80%	0.0027953	9.21	0.77865	0.0039696	184.13	0.61221	0.21606
60%	0.0031349	11.21	0.75909	0.0021683	218.8	0.56847	0.088716
40%	0.0033452	18.01	0.62091	0.0020905	229.5	0.5006	0.066692
20%	0.0039584	14.92	0.65745	0.0020599	199.4	0.38122	0.12304
0%	0.0046775	10.12	0.70804	0.0025044	152.2	0.29418	-

Table 2. EEC parameter proposal.

Parameter	Unit	Range [1]
R_1	Ω	[0.00271760, 0.00467750]
L_1	H	$[10^{-6}, 10^{-3}]$
R_2	Ω	[0.00205990, 0.00921740]
T_1	$\sec^{p1}\cdot\Omega^{-1}$	[7.17, 18.01]
p_1	-	[0.62091000, 0.85729000]
R_3	Ω	[0.06669200, ∞)
T_2	$\sec^{p1}\cdot\Omega^{-1}$	[87.18, 229.50]
p_2	-	[0.29418000, 0.65421000]

[1] In this table, we list the proposed EEC parameters. The range for each parameter is a value span within which the parameter can reasonably be found. The maximum and the minimum values of these ranges are fixed by the experimental data.

To compare the results of this new algorithm, we propose using the same equivalent circuit and tests presented in the work by Olarte et al. [22].

2.1. Electrical Equivalent Circuit Proposal

We propose the EEC in Figure 1a because the real data the battery essays produced, as described in Section 3, fit well with two pairs of constant phase elements in parallel with a resistor. The outputs of the real experiments (in black) with the theoretical model predictions obtained with Zview are shown in Figure 1b (in green). The model obtained

using Zview requires expert human supervision. The physical meanings of the EEC parameters are described in [23]. Here, R_1 is the inner resistance, R_2 is the charge transfer resistance for the negative electrode, CPE_1 is associated with a distribution of relaxation times, and CPE_2 is an impedance related to higher time constants than CPE_1. Finally, R_3 is the resistance associated with the charge transfer resistance for the positive electrode.

Table 3. EEC variables.

Variable [2]	Unit	Definition
j	-	Imaginary unit number
w	rad/s	Frequency
$EIS(jw)$	Ω	Electrochemical impedance Spectrum of the battery
$CPE_1(jw)$	Ω	First constant-phase element
$CPE_2(jw)$	Ω	Second constant-phase element
Z_{CPE_1,R_2}	Ω	Equivalent parallel impedance of first constant element and the second resistance
Z_{CPE_2,R_3}	Ω	Equivalent parallel impedance of second constant element and third resistance

[2] In this table, we list the proposed EIS equivalent circuit's main variables.

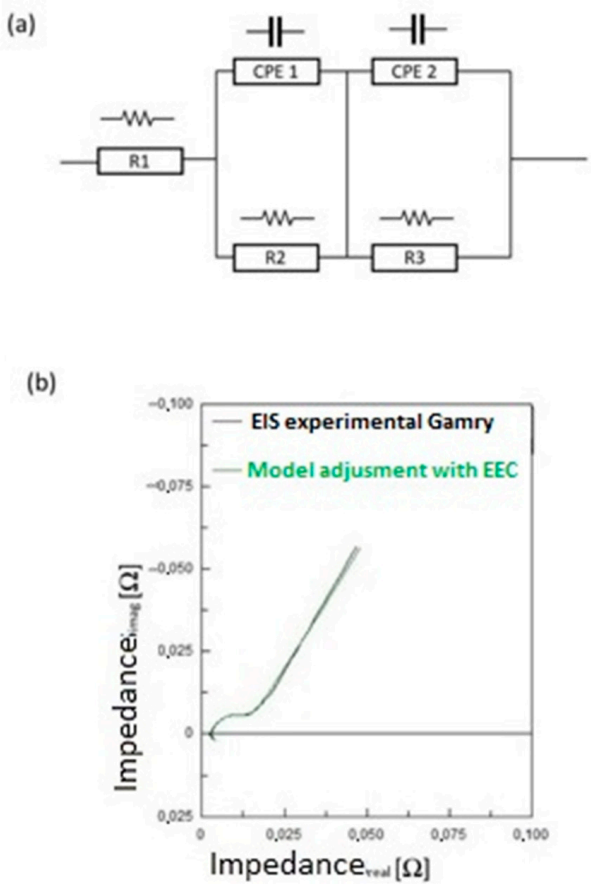

Figure 1. (**a**) Proposed EEC circuit model and (**b**) adjustment of EIS spectra of 12 V block at 100% of the state of charge (SoC) using Zview (version 3.5i) manual software.

Table 1 shows the reference parameters extracted from the EIS spectra of a lead–acid battery analyzed by adjusting the Zview manual software. These reference parameters are considered to generate the synthetic data.

The mathematical model is defined via Equations (1)–(3):

$$EIS(jw) = R_1 + jL_1w + Z_{CPE_1,R_2} + Z_{CPE_2,R_3} \tag{1}$$

$$Z_{CPE_1,R_2} = \frac{R_2 CPE_1(jw)}{CPE_1(jw) + R_2} \tag{2}$$

$$Z_{CPE_2,R_3} = \frac{R_3 CPE_2(jw)}{CPE_2(jw) + R_3} \tag{3}$$

The constant phase elements' impedances are defined in Equations (4) and (5):

$$CPE_1(jw) = \frac{1}{T_1(jw)^{p_1}} \tag{4}$$

$$CPE_2(jw) = \frac{1}{T_2(jw)^{p_2}} \tag{5}$$

Figure 1a shows the selected electrical equivalent circuit. The inductive (see L_1) parts do not contain valuable information about the battery degradation process because they are very dependent on the electrical setup, so they are not considered.

Conceptually, it is good practice to derive all expressions of impedance in the real and imaginary parts because the current automatic differentiation algorithms do not support complex variable operations:

$$real(CPE_1) = \frac{\cos\left(\frac{\pi}{2}p_1\right)}{\mathrm{T_1 w}^{p_1}} \tag{6}$$

$$imag(CPE_1) = \frac{\sin\left(\frac{\pi}{2}p_1\right)}{\mathrm{T_1 w}^{p_1}} \tag{7}$$

$$real(CPE_2) = \frac{\cos\left(\frac{\pi}{2}p_2\right)}{\mathrm{T_2 w}^{p_2}} \tag{8}$$

$$imag(CPE_2) = \frac{\sin\left(\frac{\pi}{2}p_2\right)}{\mathrm{T_2 w}^{p_2}} \tag{9}$$

$$real\left(Z_{CPE_1,R_2}\right) = \frac{\mathrm{R_2}\cdot\left(real(CPE_1)(\mathrm{R_2} + real(CPE_1)) + imag^2(CPE_1)\right)}{(\mathrm{R_2} + real(CPE_1))^2 + imag^2(CPE_1)} \tag{10}$$

$$imag\left(Z_{CPE_1,R_2}\right) = \frac{\mathrm{R_2}\cdot imag(CPE_1)((\mathrm{R_2} + real(CPE_1)) - real(CPE_1))}{(\mathrm{R_2} + real(CPE_1))^2 + imag^2(CPE_1)} \tag{11}$$

$$real\left(Z_{CPE_2,R_3}\right) = \frac{\mathrm{R_3}\cdot\left(real(CPE_2)(\mathrm{R_3} + real(CPE_2)) + imag^2(CPE_2)\right)}{(\mathrm{R_3} + real(CPE_2))^2 + imag^2(CPE_2)} \tag{12}$$

$$imag\left(Z_{CPE_2,R_3}\right) = \frac{\mathrm{R_3}\cdot imag(CPE_2)((\mathrm{R_3} + real(CPE_2)) - real(CPE_2))}{(\mathrm{R_3} + real(CPE_2))^2 + imag^2(CPE_2)} \tag{13}$$

The whole impedance can be derived via Equations (14) and (15).

$$real(EIS) = \mathrm{R_1} + real\left(Z_{CPE_1,R_2}\right) + real(Z_{CPE_2,R_3}) \tag{14}$$

$$imag(EIS) = \mathrm{L_1}w + imag\left(Z_{CPE_1,R_2}\right) + imag(Z_{CPE_2,R_3}) \tag{15}$$

2.2. Supervised Versus Unsupervised Strategies

We propose a new unsupervised training algorithm. The usual approach is to train the artificial neural network with EIS empirical data as inputs and EEC parameters as outputs, as seen in Figure 2. This approach has the disadvantages of the high costs and time periods required to obtain a sufficient dataset for training. In this research, we produced essays for 5 months. Each month, the batteries were charged and discharged at different SoCs. The costs of these essays were for the research personnel, the battery sets, the laboratory spaces, and the measuring equipment and refrigeration systems' amortization. The process produced only 36 essays, including six different SoC levels (100% to 20%) and six different times (from the start to the fifth month). Therefore, the essay measurements were expensive and time-consuming. Each impedance measurement produced an EIS essay. Due to these time and budget limitations, the amount of data was limited to 36 essays. As seen in Equation (17), $P_{ANN}(EIS_q(jw,\theta)$ is an artificial neural network that predicts the EEC parameters:

$$\vec{P} = [R_1\ L_1\ R_2\ T_1\ p_1\ R_3\ T_2\ p_2]^t \tag{16}$$

$$\vec{P}_{ANN} = \vec{P}_{ANN}(EIS_q(jw,\vec{\theta}) \tag{17}$$

$$MSE_{Loss}\left(\vec{\theta}\right) = \sum_{q=1}^{q=N_{patterns}} \sum_{\mu=1}^{\mu=N_{frequency}} \left|\vec{P}_q - P_{ANN}(EIS_q(jw_\mu,\vec{\theta}))\right|^2 \tag{18}$$

$$EIS_{model}\left(jw,\vec{P}\right) = \mathrm{R}_1 + j\mathrm{L}_1 w + Z_{CPE_1,R_2} + Z_{CPE_2,R_3} \tag{19}$$

$$MSE_{Loss}\left(\vec{\theta}\right) = \sum_{q=1}^{q=N_{patterns}} \sum_{\mu=1}^{\mu=N_{frequency}} \left|real\left(EIS_q(jw_\mu)\right) - real\left(EIS_{model}\left(jw_\mu,\vec{P}\right)\right)\right|^2 +$$

$$\sum_{q=1}^{q=N_{patterns}} \sum_{\mu=1}^{\mu=N_{frequency}} \left|imag\left(EIS_q(jw_\mu)\right) - imag\left(EIS_{model}\left(jw_\mu,\vec{P}\right)\right)\right|^2 \tag{20}$$

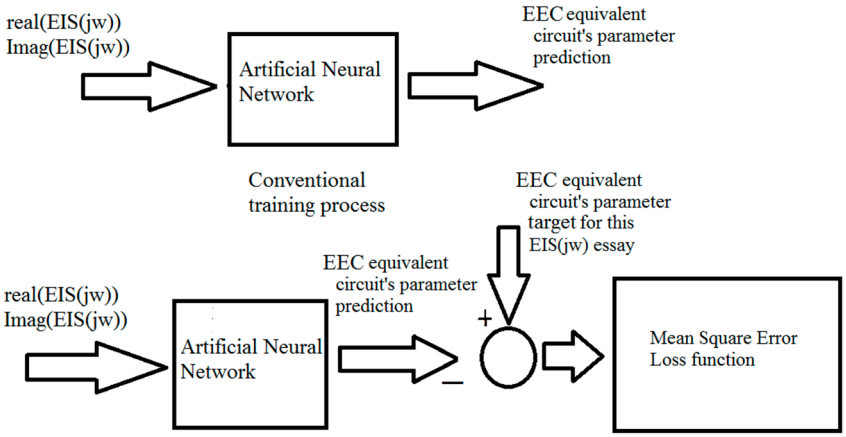

Figure 2. Supervised training model.

We propose a different mean loss function (an unsupervised training method) to reduce the prediction error, as shown in Figure 3. Table 4 defines the main variables of the EEC neural network predictor, including the inputs and outputs.

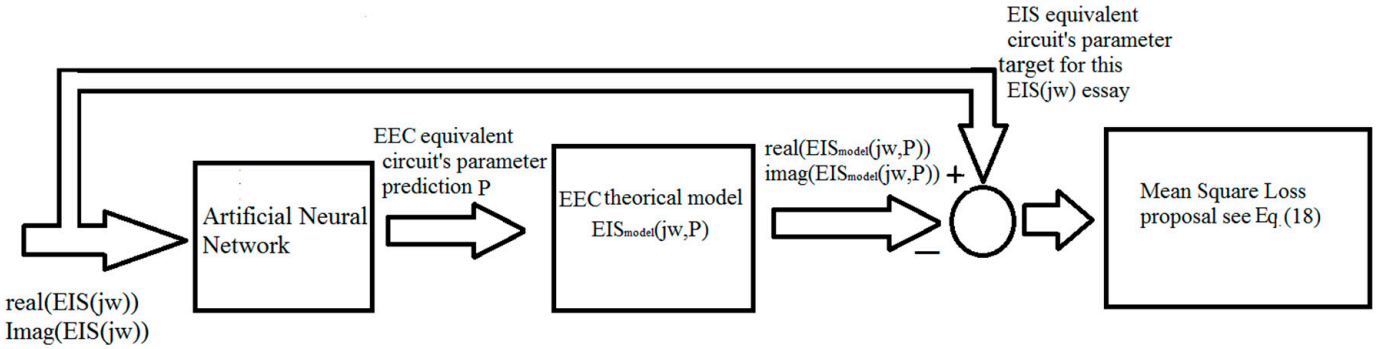

Figure 3. Unsupervised training model.

Table 4. The parameters of the proposed neural network for EEC parameter predictions. These parameters are defined in the electrical scheme in Figure 1a.

Parameter	Unit	Range	Definition
$real\left(EIS\left(jw_\mu\right)\right)$	-	[0, 1]	It is a 121-term input vector. It contains the real part of $EIS\left(jw_\mu\right)$, and these inputs are normalized.
$imag\left(EIS\left(jw_\mu\right)\right)$	-	[0, 1]	It is a 121-term input vector. It contains the imaginary part of $EIS\left(jw_\mu\right)$, and these inputs are normalized.
R_1	Ω	[0, 1]	The first resistance. The value is normalized.
L_1	H	[0, 1]	The serial inductance. The value is normalized.
R_2	Ω	[0, 1]	The second resistance. It is in parallel with the first constant-phase element.
T_1	$\sec^{p1}\cdot\Omega^{-1}$	[0, 1]	The inverse gain of the first constant-phase element. It is a normalized value.
p_1	-	[0, 1]	The power index parameter of the first constant-phase element. It is a normalized value.
R_3	Ω	[0, 1]	The third resistance. It is in parallel with the second constant-phase element. It is a normalized value.
T_2	$\sec^{p1}\cdot\Omega^{-1}$	[0, 1]	The inverse gain of the second constant-phase element. It is a normalized value.
p_2	-	[0, 1]	The power index parameter of the second constant-phase element. It is a normalized value.
w_μ	rad/sec	[0.0628, 63323] with an exponential step of Δw_μ	The frequency sample. There are 121 different frequency samples.
Δw_μ	rad/sec	$\Delta w_\mu = e^{\frac{15\mu}{N_{frequency}}-5}$	The frequency sampling step. $\mu \in \left\{0, 1, 2, \ldots, N_{frequency}\right\}$

2.3. Data Augmentation Proposal

We have proposed a data augmentation algorithm to generate synthetic training from five essays with different states of charge (SoCs) from 20% to 100% (see Table 1 for the whole set of essays used).

The generation process is defined in Algorithm 1. The objective is to generate three different datasets: a training dataset with 20,000 synthetic equivalent circuits, a validation dataset of 2500 synthetic equivalent circuits, and a test dataset of 500 synthetic equivalent circuits. The difference between the EIS values of a selected experimental essay and the synthetic equivalent circuit is defined as the absolute value of the difference between these two EIS values, which is divided by the absolute value of the selected experimental essay's EIS value (see line 9 in Algorithm 1). The maximum accepted difference level is equal to 30%. The records of each dataset were randomly selected.

Algorithm 1: Data augmentation process for synthetic essay generation

Inputs:
The set of essays with each parameter set. There are 5 different essays, with different SoCs.

- $EIS_{\mu}(jw)$, $\mu \in \{20\%, 40\%, 60\%, 80\%, 100\%\}$
- $EquivalentCircuitParameter_{\mu} = [R_1\mu, R_2\mu, R_3\mu, T_1\mu, p_1\mu, T_2\mu, p_2\mu, L_1\mu]$

The number of essays generated.

- $N_{generatedEIS}$

The maximum difference level.

- J_{max}

Outputs:
The set of synthetic essays. There are $N_{generatedEIS}$ different essays.

- $EISsynthetic,q(jw)$, $q \in \{1, NgeneratedEIS\}$
- $EquivalentCircuitParameter_q = [R_1q, R_2q, R_3q, T_1q, p_1q, T_2q, p_2q, L_1q]$

1: **procedure**
2: Obtain the maximum and the minimum values of each EEC parameter. These values are calculated from $EquivalentCircuitParameter_{\mu}$.

- $R_1max, R_2max, R_3max, T_1max, p_1max, T_2max, p_2max, L_1max$
- $R_1min, R_2min, R_3min, T_1min, p_1min, T_2min, p_2min, L_1min$

3: **for** q **from** 1 **to** $N_{generatedEIS}$
4: NextCircuit = False
5: **while not** NextCircuit
6: $\mu_{selected}$ = mod(μ,Cardinal(μ))
7: Generate an equivalent parameter set ($CircuitParameter_q$) based on $EquivalentCircuitParameter_{\mu selectced}$,
The parameters are calculated with a pseudorandom uniform value between the maximum and the minimum values calculated in line 2.
8: Generate synthetic EISsynthetic,q(jw). See Equation (1).
9: Calculate difference level as follows:

$$J = 100 \sum_{\mu=1}^{\mu=N_{frequency}} \frac{\left|EISsynthetic,q(jw_{\mu}) - EIS\mu selected(jw_{\mu})\right|}{\left|EIS\mu selected(jw_{\mu})\right|}$$

10: **if** $J < Jmax$
11: NextCircuit=True
12: **end if**
13: Store EISsynthetic,q(jw), and Store Equivalent $CircuitParameter_{\mu selectced}$
14: **end while**
15: **end for**
16: **return** EISsynthetic, q(jw), $CircuitParameter_q$, $q \in \{1, NgeneratedEIS\}$

3. Materials and Methods

The data used in this work were based on the aging and measurements of a set of 80–100 Ah and 12 V lead–acid batteries. The testing protocol included a CC charge stage and a CV charge stage. Periodic impedance measurements were performed at different state-of-charge levels, at each Δh% = 20 in the discharge process. At each SOC level, a 12 h relaxation time was established before performing the impedance measurement, which was conducted under an excitation current of 50 mA and in the frequency range of 10 mHz to 10 kHz.

As already outlined in Section 2, the EIS spectra extracted from the test were adjusted to a specific EEC to identify an EEC parameter. The proposed neural network's architecture has two inputs, where the first input is the real part of the EIS spectra and the second input is the imaginary part of the EIS spectra, with each input having 121 frequency samples. These two inputs are concatenated in one feature vector. After this concatenation, there is a fully connected layer with 100 neurons and a ReLU layer. After this, there are three blocks of fully connected layers with a ReLU layer of 10 neurons. Finally, there is a fully connected layer and a sigmoid layer of eight neurons. The output layer has eight neurons

because the artificial neuron network has to predict the parameters of the equivalent circuit (see Equation (16)). The architecture has 25,600 learnable parameters. In Figures 4 and 5, we have attached a description of the whole architecture.

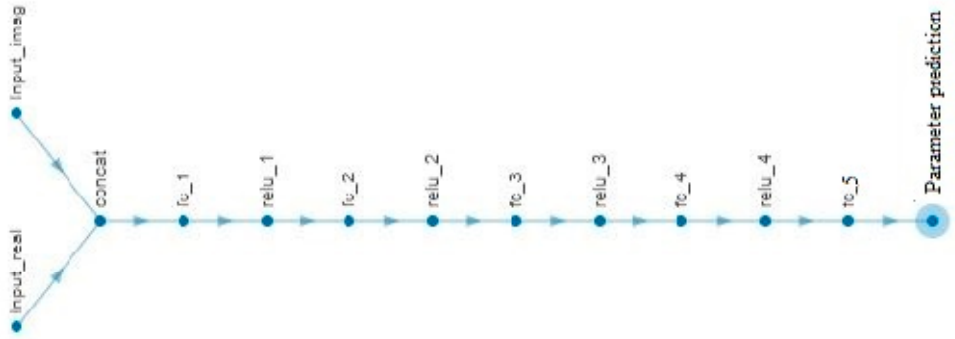

Figure 4. The proposed architecture with a directional acyclical graph of the proposed neural network.

	Name	Type	Activations	Learnable weigths
1	Input_real 121 features	Feature Input	121(C) × 1(B)	-
2	Input_imag 121 features	Feature Input	121(C) × 1(B)	-
3	concat Concatenation of 2 inputs along dimensi...	Concatenation	242(C) × 1(B)	-
4	fc_1 100 fully connected layer	Fully Connected	100(C) × 1(B)	Weights 100 × 242 Bias 100 × 1
5	relu_1 ReLU	ReLU	100(C) × 1(B)	-
6	fc_2 10 fully connected layer	Fully Connected	10(C) × 1(B)	Weights 10 × 100 Bias 10 × 1
7	relu_2 ReLU	ReLU	10(C) × 1(B)	-
8	fc_3 10 fully connected layer	Fully Connected	10(C) × 1(B)	Weights 10 × 10 Bias 10 × 1
9	relu_3 ReLU	ReLU	10(C) × 1(B)	-
10	fc_4 10 fully connected layer	Fully Connected	10(C) × 1(B)	Weights 10 × 10 Bias 10 × 1
11	relu_4 ReLU	ReLU	10(C) × 1(B)	-
12	fc_5 8 fully connected layer	Fully Connected	8(C) × 1(B)	Weights 8 × 10 Bias 8 × 1
13	Parameter prediction sigmoid	Sigmoid	8(C) × 1(B)	-

Figure 5. Summary information of each layer of the proposed neural network.

The training process is an ADAM algorithm with 60 epochs, with a mini-batch size of 100 synthetic circuits. The initial learning ratio is equal to 10^{-3}. The gradient decay factor is set to 0.9 and the squared decay factor is set to 0.999. The epsilon value (small constant) is set to 10^{-8}.

4. Results

We compared the normalized theoretical EIS data with the EIS data generated using the parameters predicted by the neural network. We plotted the theoretical EIS data (in red) calculated using Equations (1)–(5) with the EEC parameter predicted by the neural network. When the neural network takes an experimental EIS datum as an input, it predicts the EEC parameter set (see Table 1). We trained the neural network to predict parameters to match the experimental EIS data via Equations (1)–(5), not the EEC parameters. In Figure 6, the axes are the normalized real parts of the EIS data (x-axis) and the imaginary parts of the EIS data (y-axis). The figures do not have units because the real parts were normalized from [0 to 1] and the imaginary parts from [−1 to 0]. The scales were normalized with the

experimental maximum and minimum values. We used the relative error of the normalized EIS data (see Equation (21)).

$$J_{relative\ error} = 100 \sum_{\mu=1}^{\mu=N_{frequency}} \frac{\left|EISpredictedANN(jw_\mu) - EISinput(jw_\mu)\right|}{\left|EISinput(jw_\mu)\right|} \quad (21)$$

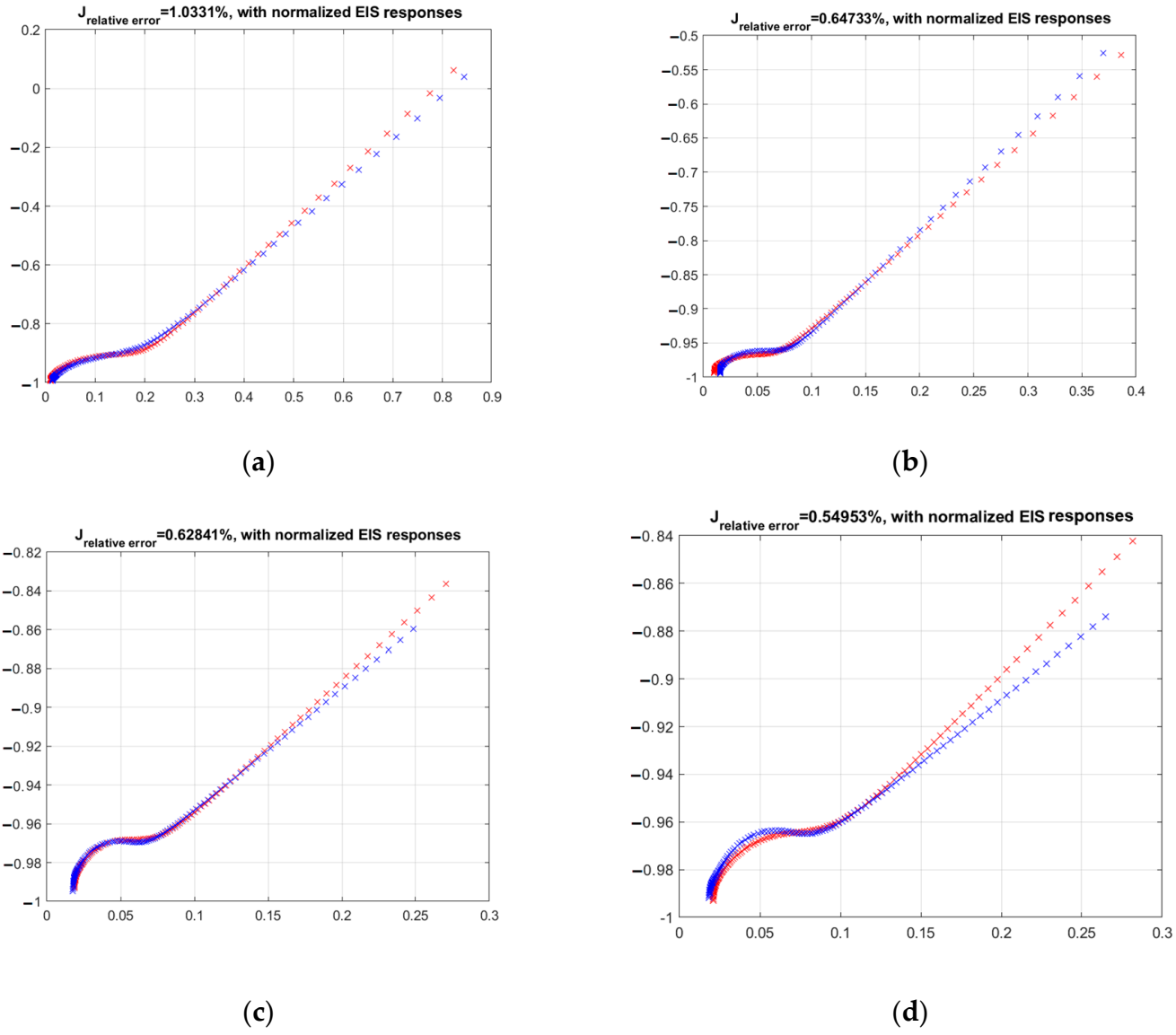

Figure 6. (**a**,**b**) Comparisons between the theoretical EIS data (in red) with the parameter set predicted by the neural network and the normalized EIS data (in blue) given to the artificial neural network. (**c**,**d**) The worst cases for the neural network predictions. The performance results are the relative mean square errors between the spectra generated with the parameters predicted by the neural network and the spectra of the EIS input data.

5. Discussion

To calculate the electrical parameters from measured EIS data, we proposed a feedforward neural network fed with synthetic data generated from a small amount of manually adjusted EIS experimental data. This neural network consists of a series of layers, with the first one being the input layer (mapped onto the EIS data) and the last one being the output layer (mapped onto the EEC parameters). It is proposed that one neural network be trained to predict each one of the parameters corresponding to the eight parameters of the selected EEC circuit. The layers contained between the input and the output are the hidden layers.

For the selected EEC and with the experimental data obtained from laboratory tests, it has been proven that the new unsupervised algorithm based on deep learning obtains better results as an automatic estimator of an equivalent circuit's parameters based on EIS data compared with supervised training approaches, as previously reported by the authors in [14].

The proposed data augmentation process based on synthetic equivalent circuits is a good method to create realistic solutions regarding the experimental data. This technique can generate many synthetic EIS datapoints based on a few known experimental EIS datapoints.

The proposed neural network can be applied as an abnormality detector when the predicted EEC parameter values create very different results from the input EIS data. On the one hand, the proposed neural network can provide EIS equivalent circuit parameters, while on the other hand it can predict unusual EIS values and consequently detect abnormal behaviors. Therefore, this neural network can detect when predictions are too far from the input EIS data so that a new training process can be executed.

The neural network, data augmentation process, and new training loss function can be applied to identify the parameters of any transfer function in other applications. The neural network can predict transfer function coefficients using the Fourier response of a linear dynamic system. In the authors' opinion, this capability shows that this is a powerful technique to create a neural network that identifies a transfer function.

6. Conclusions

The most important outcome of this work is that a new loss function has been proposed to identify a battery's EEC parameters (see Equation (21) and Figure 3). In future research, we propose that regularization techniques L1 and L2 are developed to select a battery model that is complex enough to explain the spectrum data and simple enough to avoid overfitting.

Our loss function proposal applies to other electrochemical batteries. It is essential to propose a sufficiently general circuit for the loss function. This technique can be applied to other models. A very complex model can be proposed with many constant-phase elements in parallel with a resistor. The overfitting problems of the model decrease when using L1 or L2 regularization techniques. As such, only the most relevant elements of the model are changed from zero. Therefore, this loss function can be applied to select an EEC model that is complex enough to explain the EIS spectrum data and simple enough to avoid overfitting. In [24], one can determine how different EEC parameters must be defined for different temperatures for Li_6PS_5Cl and other electrochemistry technologies. The proposed work can define different EEC parameters to identify the most significant models. Therefore, the researcher can automatically select parameters via the training process, thereby introducing different EEC parameters into the loss function. The training data must be increased with these new EEC parameters to obtain enough data to classify different EEC circuits. The EIS changes with different aging effects such as the temperature or discharge cycles and discharge depth, which are all operational conditions. In this paper, we have proposed a new loss function to improve the EEC parameter identification process with very few essays. In our future research, we will study the real relationship between the SoH and the identified EEC parameters. The trained neural network can detect changes in the EIS behavior if the different EIS shapes can be explained with the same model architecture. In this study, the proposed architecture could explain all EIS variations. Furthermore, the proposed loss function can be extended to more general models or more than one model simultaneously, although the neural network architecture must be changed to predict a new EEC parameter set by applying the training loop in the same way.

Author Contributions: Conceptualization, A.Z. and E.Z.; methodology, A.Z.; software, E.Z., A.Z. and S.E.; validation, J.O. and U.F.-G.; formal analysis, A.Z.; investigation, J.M.L.-G. and J.O.; resources, U.F.-G. and E.Z.; writing—original draft preparation, A.Z., J.O. and E.Z.; writing—review and editing E.Z., U.F.-G. and J.O. All authors have read and agreed to the published version of the manuscript.

Funding: The authors were supported by the Mobility Lab Foundation, a governmental organization of the Provincial Council of Araba and the local council of Vitoria-Gasteiz under the project grant of "Control de baterías de flujo".

Data Availability Statement: Data are contained within the article.

Acknowledgments: The authors recognize the collaboration of the Bcare company for lending their laboratory materials and essays to develop this research.

Conflicts of Interest: The authors declare no conflict of interest.

References

1. Plett, G.L. *ECE4710/5710: Modeling Simulation and Identification of Battery Dynamics Equivalent-Circuit Cell Models*; University of Colorado Springs: Colorado Springs, CO, USA, 2011. Available online: http://Mocha-Java.Uccs.Edu/ECE5710/ECE5710-Notes02.pdf (accessed on 10 October 2023).
2. Costa, N.; Sánchez, L.; Anseán, D.; Dubarry, M. Li-ion battery degradation modes diagnosis via Convolutional Neural Networks. *J. Energy Storage* **2022**, *55*, 105558. [CrossRef]
3. Xu, R.; Wang, Y.; Chen, Z. Data-driven battery aging mechanism analysis and degradation pathway prediction. *Batteries* **2023**, *9*, 129. [CrossRef]
4. Zhang, Y.; Xiong, R.; He, H.; Pecht, M.G. Long short-term memory recurrent neural network for remaining useful life prediction of lithium-ion batteries. *IEEE Trans. Veh. Technol.* **2018**, *67*, 5695–5705. [CrossRef]
5. Gasper, P.; Schiek, A.; Smith, K.; Shimonishi, Y.; Yoshida, S. Predicting battery capacity from impedance at varying temperature and state of charge using machine learning. *Cell Rep. Phys. Sci.* **2022**, *3*, 101184. [CrossRef]
6. Omariba, Z.B.; Zhang, L.; Kang, H.; Sun, D. Parameter identification and state estimation of lithium-ion batteries for electric vehicles with vibration and temperature dynamics. *World Electr. Veh. J.* **2020**, *11*, 50. [CrossRef]
7. Ren, Z.; Du, C. A review of machine learning state-of-charge and state-of-health estimation algorithms for lithium-ion batteries. *Energy Rep.* **2023**, *9*, 2993–3021. [CrossRef]
8. Lombardo, T.; Duquesnoy, M.; El-Bouysidy, H.; Årén, F.; Gallo-Bueno, A.; Jørgensen, P.B.; Bhowmik, A.; Demortière, A.; Ayerbe, E.; Alcaide, F.; et al. Artificial intelligence applied to battery research: Hype or reality? *Chem. Rev.* **2021**, *122*, 10899–10969. [CrossRef]
9. Alavi, S.M.; Birklm, C.R.; Howey, D.A. Time-domain fitting of battery electrochemical impedance models. *J. Power Sources* **2015**, *288*, 345–352. [CrossRef]
10. Pastor-Fernández, C.; Uddin, K.; Chouchelamane, G.H.; Widanage, W.D.; Marco, J. A comparison between electrochemical impedance spectroscopy and incremental capacity-differential voltage as Li-ion diagnostic techniques to identify and quantify the effects of degradation modes within battery management systems. *J. Power Sources* **2017**, *360*, 301–318. [CrossRef]
11. Choi, W.; Shin, H.-C.; Kim, J.M.; Choi, J.-Y.; Yoon, W.-S. Modeling and applications of electrochemical impedance spectroscopy (EIS) for lithium-ion batteries. *J. Electrochem. Sci. Technol.* **2020**, *11*, 1–13. [CrossRef]
12. Olarte, J.; de Ilarduya, J.M.; Zulueta, E.; Ferret, R.; Fernández-Gámiz, U.; Lopez-Guede, J.M. A battery management system with EIS monitoring of life expectancy for lead–acid batteries. *Electronics* **2021**, *10*, 1228. [CrossRef]
13. Piller, S.; Perrin, M.; Jossen, A. Methods for state-of-charge determination and their applications. *J. Power Sources* **2001**, *96*, 113–120. [CrossRef]
14. Meddings, N.; Heinrich, M.; Overney, F.; Lee, J.-S.; Ruiz, V.; Napolitano, E.; Seitz, S.; Hinds, G.; Raccichini, R.; Gaberšček, M.; et al. Application of electrochemical impedance spectroscopy to commercial Li-ion cells: A review. *J. Power Sources* **2020**, *480*, 228742. [CrossRef]
15. Csomos, B.; Fodor, D. Identification of the Material Properties of an 18650 Li-Ion Battery for Improving the Electrochemical Model used in Cell Testing. *Hung. J. Ind. Chem.* **2020**, *48*, 33–41. [CrossRef]
16. Song, K.; Hu, D.; Tong, Y.; Yue, X. Remaining life prediction of lithium-ion batteries based on health management: A review. *J. Energy Storage* **2023**, *57*, 106193. [CrossRef]
17. Attia, P.M.; Bills, A.; Planella, F.B.; Dechent, P.; Dos Reis, G.; Dubarry, M.; Gasper, P.; Gilchrist, R.; Greenbank, S.; Howey, D.; et al. "Knees" in lithium-ion battery aging trajectories. *J. Electrochem. Soc.* **2022**, *169*, 060517. [CrossRef]
18. Chun, H.; Kim, J.; Han, S. Parameter identification of an electrochemical lithium-ion battery model with convolutional neural network. *IFAC-PapersOnLine* **2019**, *52*, 129–134. [CrossRef]
19. Zhang, S.; Hosen, S.; Kalogiannis, T.; Van Mierlo, J.; Berecibar, M. State of health estimation of lithium-ion batteries based on electrochemical impedance spectroscopy and backpropagation neural network. *World Electr. Veh. J.* **2021**, *12*, 156. [CrossRef]
20. Jiménez-Bermejo, D.; Fraile-Ardanuy, J.; Castaño-Solis, S.; Merino, J.; Álvaro-Hermana, R. Using dynamic neural networks for battery state of charge estimation in electric vehicles. *Procedia Comput. Sci.* **2018**, *130*, 533–540. [CrossRef]
21. Yang, D.; Wang, Y.; Pan, R.; Chen, R.; Chen, Z. A neural network based state-of-health estimation of lithium-ion battery in electric vehicles. *Energy Procedia* **2017**, *105*, 2059–2064. [CrossRef]
22. Olarte, J.; de Ilarduya, J.M.; Zulueta, E.; Ferret, R.; Fernández-Gámiz, U.; Lopez-Guede, J.M. Automatic identification algorithm of equivalent electrochemical circuit based on electroscopic impedance data for a lead acid battery. *Electronics* **2021**, *10*, 1353. [CrossRef]

23. Badeda, J.; Kwiecien, M.; Schulte, D.; Sauer, D.U. Battery state estimation for lead-acid batteries under float charge conditions by impedance: Benchmark of common detection methods. *Appl. Sci.* **2018**, *8*, 1308. [CrossRef]
24. Xu, H.; Cao, G.; Shen, Y.; Yu, Y.; Hu, J.; Wang, Z.; Shao, G. Enabling Argyrodite Sulfides as Superb Solid-State Electrolyte with Remarkable Interfacial Stability Against Electrodes. *Energy Environ. Mater.* **2022**, *5*, 852–864. [CrossRef]